Synthesis and Characterization of Poly(fluorene)-Based Copolymers Containing Various 1,3,4-Oxadiazole Dendritic Pendants

Chung-Wen Wu, Chien-Min Tsai, and Hong-Cheu Lin*

Department of Materials Science and Engineering, National Chiao Tung University, Hsinchu, Taiwan (ROC)

Received April 3, 2006; Revised Manuscript Received April 26, 2006

ABSTRACT: A series of poly(fluorene)s (PFs) containing different generations of poly(benzyl ether) dendritic wedges with oxadiazole (OXD) peripheral functional groups, including copolymers bearing carbazole (CAZ) pendent groups, were synthesized. The dendritic side-chain polymers possessed excellent solubility in common solvents and good thermal stability with decomposition temperatures of 5% weight loss at more than 370 °C. Photophysical studies reveal that the photoluminescent (PL) properties of the dendronized polymers were greatly affected by the size of the dendritic side chains. The G1- and G2-substituted PF derivatives greatly suppress the aggregation PF backbones and thus to induce pure blue PL emission (with shorter wavelengths than PF). Excitation of the peripheral functional groups leads to substantial energy transfer from the dendrons to the poly(fluorene) backbones. In addition, the excitation of PF bearing G2 dendrons (G2-OXD) at 303 nm creates stronger fluorescence than that at 390 nm, indicating that the intensity of the sensitized emission (by OXD absorption at 303 nm) is even stronger than that of a direct poly(fluorene) emission (by PF backbone absorption at 390 nm). Double-layer light-emitting diode (LED) devices with the configuration of ITO/PEDOT/polymer/LiF/Al were fabricated and reported. The device with PF bearing G0 dendrons and CAZ pendants (G0-OXDCAZ) as an emitter shows a turn-on voltage of 4.5 V and a bright luminescence of 2446 cd/m^2 at 12 V with a power efficiency of 0.24 cd/A at 100 mA/cm^2.

Introduction

π-Conjugated materials with electronically rigid backbones have attracted considerable interest in both academic research and industrial applications due to increasing potential as active components for a wide range of electronic and optoelectronic devices.[1] In the past decade, fluorene-based conjugated polymers have emerged as a very outstanding class of blue-light emitting materials because of their high photoluminescence (PL) and electroluminescence (EL) quantum efficiencies, thermal stability, good solubility, high hole mobility, and facile functionalization at the C-9 position of fluorene.[2] However, devices are restricted by their tendency to form aggregates,[3] excimers,[4] or ketone defects[5] during either annealing or passage of current, leading to red-shifted and less efficient emissions. To avoid this detrimental behavior, a number of approaches have been used. One approach is to introduce end-capped poly(fluorene)s (PFs) with bulky groups,[6,7] spirofluorene functionalized bifluorene moieties,[8,9] networking poly(fluorene)s,[10] and dendritic side groups into the C-9 position of poly(fluorene)s[11] as well as minimization of isolated fluorenone defects.[12]

To obtain highly efficient light emitting devices, a balance in the injection and transportation of both holes and electrons into the polymer emissive layer is necessary.[13−17] However, most electroluminescent polymers inject and transport holes more efficiently than electrons, which result in an unbalance of opposite carrier currents. Polymers containing electron-withdrawing units in the main chains or side chains usually have large electron affinities. 2,5-Diphenyl-1,3,4-oxadiazole (OXD) derivatives are the most widely studied classes of electron-injection and/or hole-blocking materials[18] by virtue of many merits owned by 1,3,4-OXD moieties, such as prominent electron affinity, high photoluminescence, and good thermal stability.[19] Certain poly(fluorene)s containing OXD units have been synthesized and reported recently.[20−22]

To reduce the formation of excimers and the aggregation of emitters, dendronized polymers are a promising approach to be used as multifunctional light-emitting materials. The dendrons not only protect the polymer rods from both aggregation and degradation but also tune unbalanced carrier-transporting properties, where proper charge-transporting functionalities are incorporated to the periphery of the dendrons.[23,24] Furthermore, the peripheral donor units can transfer excitation energy to the polymer backbones and enhance fluorescent properties. Here, we report a family of dendronized poly(fluorene)s bearing OXD units on the outer surface of poly(aryl ether) dendritic wedges. To determine the minimal steric requirements for prevention of aggregation, we prepared polymers bearing OXD side chains with three generations of dendrons. We hope the dendronized polymers can take advantage of the bulky OXD pendants to avoid the tendency of spontaneous aggregation and crystallization normally encountered in poly(fluorene)s, so as to show specific light-antenna capacity and tunable charge-transporting characteristics. On the other hand, the previous research[21] reported that the ionization potential of poly(fluorene) with pendant OXD units is 5.76 eV, which is similar to that of poly(9,9-dioctylfluorene) (5.8 eV). This means that there is a significant energy barrier for hole injection, and it needs to be improved in order to further enhance the device performance. It is well-known that the carbazole (CAZ) unit reduces the hole-injection barrier in poly(fluorene) in this manner, to facilitate hole injection from ITO electrodes.[25] For this reason, we also introduce hole-transporting CAZ groups to the PF backbones as pendants for a comparative investigation. The absorption, PL emission, and EL spectra were also studied to gain insight into the interaction between peripheral units and poly(fluorene) backbones.

* Author for correspondence. Telephone: 8863-5712121 ext. 55305 Fax: 8863-5724727. E-mail: linhc@cc.nctu.edu.tw.

10.1021/ma060743q CCC: $33.50
Published on Web 05/26/2006

Scheme 1. Synthetic Routes of Macromonomers (M1−M3) and Polymers (P1−P6)

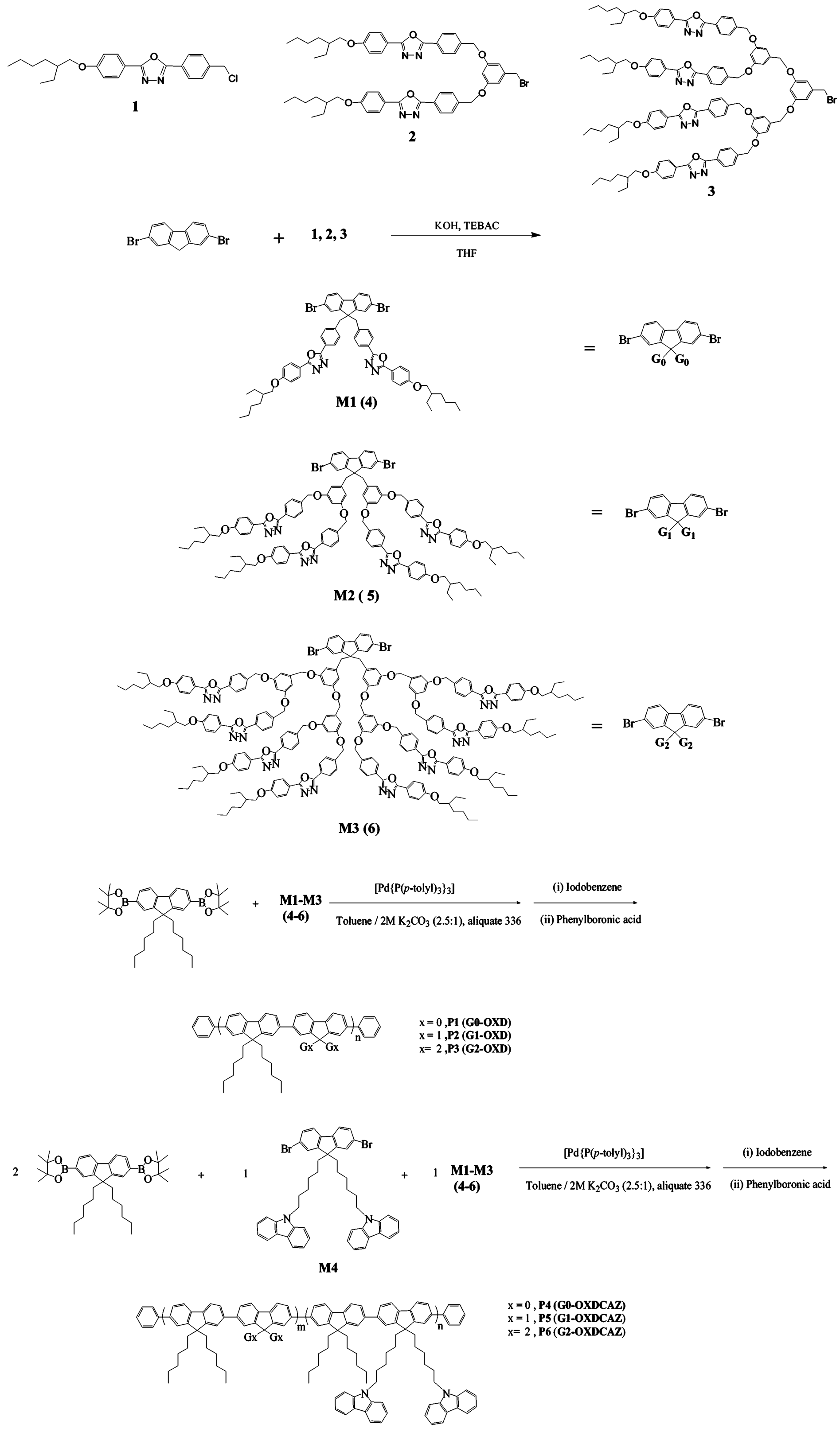

Experimental Section

Materials. 2,7-Bis(4,4,5,5-tetramethyl-1,3,2-dioxaborolan-2-yl)-9,9-dihexylfluorene[26] and 9,9-bis(4-carbazol-9-ylhexyl)-2,7-dibromofluorene (**M4**)[25] were synthesized according to literature procedures. Synthesis and characterization of compounds **1**−**3** (shown in Scheme 1) and their intermediates are described in the Supporting Information (as shown in Scheme 1 of the Supporting Information).[27] Chemicals and solvents were reagent grades and purchased from Aldrich, Acros, TCI, and Lancaster Chemical Co. Dichloromethane and THF were distilled to keep them anhydrous before use. The other chemicals were used without further purification.

General Procedure for the Synthesis of Dendronized Macromonomers. A mixture of 2,7-dibromofluorene and triethylbenzylammonium chloride (TEBAC) in THFwas degassed three times;

a 50 wt % aqueous KOH solution was added and stirred for 10 min under nitrogen. To this mixture, the solution of **1** (or **2** or **3**) was added in degassed THF under nitrogen; the reaction mixture was stirred under nitrogen for 10 h, water was added, and the aqueous layer was extracted with CH_2Cl_2. The combined organic phases were dried over $MgSO_4$. After removal of the solvent, the crude product was purified as outlined in the following text.

M1. 2,7-Dibromofluorene (0.13 g, 0.39 mmol), TEBAC (3.0 mg, 0.01 mmol), THF (140mL), aqueous KOH solution (2 mL, 50 wt %), and compound **1** (0.33 g, 0.82 mmol) were used. Chromatography on silica gel eluted with CH_2Cl_2 afforded **M1** as a white solid (0.41 g, 62%). ^{1}H NMR (ppm, $CDCl_3$): 0.87−0.94 (m, 12H), 1.24−1.53 (m, 16H), 1.69−1.75 (m, 2H), 3.46 (s, 4H), 3.88 (d, J = 5.7 Hz, 4H), 6.76 (d, J = 8.7 Hz, 4H), 6.97 (d, J = 9.0 Hz, 4H), 7.16 (d, J = 8.1 Hz, 2H), 7.35 (dd, J = 1.5, 8.4 Hz, 2H), 7.66−7.70 (overlap, 6H), 7.97 (d, J = 9.0 Hz, 4H). MS (FAB): m/z [M$^+$] 1049.3; calcd m/z [M$^+$] 1048.94. Anal. Calcd for $C_{59}H_{60}Br_2N_4O_4$: C, 67.56; H, 5.77; N, 5.34. Found: C, 67.42; H, 5.69; N, 5.26.

M2. 2,7-Dibromofluorene (0.13 g, 0.39 mmol), TEBAC (3.0 mg, 0.01 mmol), THF (140 mL), aqueous KOH solution (2 mL, 50 wt %), and compound **2** (0.76 g, 0.82 mmol) were used. Chromatography on silica gel eluted with EA/CH_2Cl_2 (2:1) afforded **M2** as a white solid (0.51 g, 65%). ^{1}H NMR (ppm, $CDCl_3$): 0.91−0.97 (m, 24H), 1.34−1.53 (m, 32H), 1.72−1.78 (m, 4H), 3.19 (s, 4H), 3.92 (d, J = 5.4 Hz, 8H), 4.82 (s, 8H), 5.91 (s, 4H), 6.29 (s, 2H), 7.02 (d, J = 9.0 Hz, 8H), 7.26 (d, J = 8.1 Hz, 2H), 7.41 (d, J = 8.1 Hz, 2H), 7.48 (d, J = 8.4 Hz, 8H), 7.58 (s, 2H), 8.05 (d, J = 9.0 Hz, 8H), 8.11 (d, J = 8.1 Hz, 8H). MS (MALDI−TOF): m/z [M$^+$] 2018.78; calcd m/z [M$^+$] 2018.11. Anal. Calcd for $C_{119}H_{124}Br_2N_8O_{12}$: C, 70.82; H, 6.19; N, 5.55. Found: C, 70.88; H, 6.27; N, 5.57.

M3. 2,7-Dibromofluorene (0.04 g, 0.1 mmol), TEBAC (0.6 mg), THF (90 mL), aqueous KOH solution (2 mL, 50 wt %), and compound **3** (0.46 g, 0.24 mmol) were used. Chromatography on silica gel eluted with THF/CH_2Cl_2 (1:5) afforded **M3** as a white solid (0.22 g, 55%). ^{1}H NMR (ppm, $CDCl_3$): 0.89−0.96 (m, 48H), 1.29−1.56 (m, 64H), 1.68−1.76 (m, 8H), 3.08 (s, 4H), 3.89 (d, J = 5.7 Hz, 16H), 4.70 (s, 8H), 5.03 (s, 16H), 5.87 (s, 4H), 6.32 (s, 2H), 6.48 (s, 4H), 6.60 (s, 8H), 6.99 (d, J = 8.4 Hz, 16H), 7.22 (d, J = 7.8 Hz, 2H), 7.32 (d, J = 8.1 Hz, 2H), 7.43 (s, 2H), 7.51 (d, J = 7.8 Hz, 16H), 8.01 (d, J = 8.4 Hz, 16H), 8.07 (d, J = 8.1 Hz, 16H). MS (MALDI−TOF): m/z [M$^+$] 3957.87; calcd m/z [M$^+$] 3956.46. Anal. Calcd for $C_{239}H_{252}Br_2N_{16}O_{28}$: C, 72.55; H, 6.42; N, 5.66. Found: C, 72.65; H, 6.41; N, 5.73.

General Procedure for the Synthesis of Dendronized Polymers P1—P6. The synthetic route of polymers is shown in Scheme 1. A general procedure of polymerization is proceeded through the Suzuki coupling reaction. For polymers **P1**−**P3**, a mixture of 2,7-bis(4,4,5,5-tetramethyl-1,3,2-dioxaborolan-2-yl)-9,9-dihexyllfluorene (1 equiv), monomer **M1** (or **M2** or **M3**) (1 equiv), and freshly prepared Pd{P(p-tolyl)$_3$}$_3$ (1.0 mol %) were added in a degassed mixture of toluene ([monomer] = 0.2 M) and aqueous 2 M potassium carbonate (3:2 in volume). The mixture was vigorously stirred at 80 °C for 72 h. After the mixture was cooled to room temperature, it was poured into 200 mL of methanol. A fibrous solid was obtained by filtration. The solid was washed sequentially with methanol, water, and methanol. A similar procedure is carried out for the synthesis of **P4**−**P6**, and the feed ratio of 2,7-bis(4,4,5,5-tetramethyl-1,3,2-dioxaborolan-2-yl)-9,9-dioctylfluorene/**M1** (or **M2** or M3)/**M4** is 2/1/1. The actual m/n ratio of the resulting polymers **P4**−**P6** is about 1:1, which is calculated from proton NMR.

P1 (G0-OXD). Yield: 87%. ^{1}H NMR (ppm, $CDCl_3$): 0.79−0.95 (m, 22H), 1.16−1.49 (m, 28H), 1.72−1.74 (m, 2H), 2.16 (br, 4H), 3.67 (br, 4H), 3.89 (d, 4H), 6.99−7.02 (m, 8H), 7.61−7.81 (m, 16H), 8.03 (d, J = 8.4 Hz, 4H). Anal. Calcd for $C_{84}H_{92}N_4O_4$: C, 82.58; H, 7.59; N, 4.59. Found: C, 81.71; H, 7.56; N, 4.06.

P2 (G1-OXD). Yield: 83%. ^{1}H NMR (ppm, $CDCl_3$): 0.64−0.94 (m, 34H), 1.32−1.49 (m, 44H), 1.70−1.72 (m, 4H), 2.09 (br, 4H), 3.40 (br, 4H), 3.86 (d, J = 5.4 Hz, 8H), 4.77 (s, 8H), 6.12 (s, 4H), 6.36 (s, 2H), 6.96 (d, J = 9.0 Hz, 8H), 7.32 (d, J = 7.5 Hz, 8H), 7.64 (m, 12H), 7.99 (d, J = 9.0 Hz, 16H). Anal. Calcd for $C_{144}H_{156}N_8O_{12}$: C, 78.94; H, 7.18; N, 5.11. Found: C, 78.21; H, 7.23; N, 4.61.

P3 (G2-OXD). Yield: 80%. ^{1}H NMR (ppm, $CDCl_3$): 0.64−0.94 (m, 58H), 1.29−1.44 (m, 76H), 1.68 (m, 8H), 2.05 (br, 4H), 3.40 (br, 4H), 3.82 (d, 16H), 4.80 (m, 24H), 6.36−6.48 (m, 18H), 6.92 (d, J = 8.1 Hz, 16H), 7.35 (d, J = 8.7 Hz, 16H), 7.64 (m, 12H), 7.92 (d, J = 9.0 Hz, 32H). Anal. Calcd for $C_{264}H_{284}N_{16}O_{28}$: C, 76.79; H, 6.93; N, 5.43. Found: C, 75.73; H, 7.01; N, 4.74.

P4 (G0-OXDCAZ). Yield: 80%. ^{1}H NMR (ppm, $CDCl_3$): 0.77−1.11 (m, 36H), 1.30−1.59 (m, 48H), 1.71 (m, 6H), 2.08 (br, 12H), 3.63 (br, 4H), 3.88 (d, 4H), 4.16 (t, 4H), 6.99 (d, J = 9.0 Hz, 8H), 7.18 (t, 4H), 7.27−7.38 (m, 8H), 7.64−7.81 (m, 28H), 8.00−8.06 (m, 8H). Anal. Calcd for $C_{158}H_{170}N_6O_4$: C, 85.59; H, 7.73; N, 3.79. Found: C, 83.78; H, 7.65; N, 3.41.

P5 (G1-OXDCAZ). Yield: 77%. ^{1}H NMR (ppm, $CDCl_3$): 0.64−0.95 (m, 48H), 1.01−1.45 (m, 64H), 1.66−1.70 (m, 8H), 2.05 (br, 12H), 3.40 (br, 4H), 3.86 (d, J = 4.8 Hz, 8H), 4.15 (t, 4H), 4.78 (s, 8H), 6.12 (s, 4H), 6.35 (s, 2H), 6.96 (d, J = 8.7 Hz, 8H), 7.13−7.38 (m, 20H), 7.65−7.80 (m, 24H), 8.01−8.04 (m, 20H). Anal. Calcd for $C_{218}H_{234}N_{10}O_{12}$: C, 82.18; H, 7.40; N, 4.40. Found: C, 81.56; H, 7.26; N, 4.20.

P6 (G2-OXDCAZ). Yield: 73%. ^{1}H NMR (ppm, $CDCl_3$): 0.70−1.08 (m, 76H), 1.31−1.46 (m, 92H), 1.69−1.71 (m, 12H), 2.05 (br, 12H), 3.40 (br, 4H), 3.84 (d, J = 5.4 Hz, 16H), 4.13 (t, 4H), 4.70−4.89 (m, 24H), 6.14 (s, 4H), 6.40−6.52 (m, 14H), 6.94 (d, J = 7.2 Hz, 16H), 7.14−7.30 (m, 12H), 7.40 (d, J = 8.7 Hz, 16H), 7.64 (m, 24H), 7.94−8.05 (m, 36H). Anal. Calcd for $C_{338}H_{362}N_{18}O_{28}$: C, 79.22; H, 7.12; N, 4.92. Found: C, 78.79; H, 7.14; N, 4.74.

Characterization. ^{1}H NMR spectra were recorded on a Varian Unity 300 MHz spectrometer using $CDCl_3$ solvent. Elemental analyses were performed on a HERAEUS CHN−OS RAPID elemental analyzer. Transition temperatures were determined by differential scanning calorimetry (Perkin-Elmer Diamond) with a heating and cooling rate of 10 °C/min. Thermogravimetric analysis (TGA) was conducted on a Du Pont Thermal Analyst 2100 system with a TGA 2950 thermogravimetric analyzer under nitrogen with a heating rate of 20 °C/min. Gel permeation chromatography (GPC) analysis was conducted on a Water 1515 separation module using polystyrene as a standard and THF as an eluant. UV−visible absorption spectra were recorded in dilute chloroform solutions (10^{-6} M) on a HP G1103A spectrophotometer, and fluorescence spectra were obtained on a Hitachi F-4500 spectrophotometer. PL excitation and emission slits in solutions were 5 and 2.5 nm, respectively. PL excitation and emission slits in solid films were both 5 nm. Electrochemistry measurements were performed using an Autolab PGSTAT30 potentiostat/galvanostat with a standard three-electrode electrochemical cell containing a 0.1 M tetrabutylammonium hexafluorophosphate solution in acetonitrile at room temperature under nitrogen at a scanning rate of 100 mV/s. A platinum working electrode, a platinum wire counter electrode, and an Ag/AgCl reference electrode were used. The onset potentials were determined from the intersection of two tangents drawn at the rising current and background current of the cyclic voltammogram. Polymer solid films were spin-coated on quartz substrates from THF solutions with a concentration of 10 mg/mL.

EL Device Fabrication. The devices were fabricated on ITO substrates that had been ultrasonicated and sequentially washed in detergent, methanol, 2-propanol, and acetone and further treated with O_2 plasma for 10 min before use. A thin layer of PEDOT (40 nm) and polymers (70−100 nm) (from a 15 mg/mL solution of the polymers in dichloroethane solution) was spin-coated on the ITO surface, after which a thin layer of LiF(1 nm)/Al(100 nm) was deposited on the polymer film by thermal evaporation under a vacuum of 10^{-6} Torr. The luminance−current−voltage characteristics were recorded on a power source (Keithley 2400) and photometer (MINOLTA CS-100A).

Results and Discussion

Synthesis and Characterization. The chemical structures of dendronized macromonomers **M1-M3** are shown in

CDV

Table 1. Molecular Weights and Thermal Properties of Polymers

polymer	M_n[a]	M_w[a]	PDI	T_g[b] (°C)	T_d[c] (°C)
P1 (G0-OXD)	34 500	102 600	2.97	143	372
P2 (G1-OXD)	35 600	66 700	1.87	102	395
P3 (G2-OXD)	21 300	29 000	1.36	87	405
P4 (G0-OXDCAZ)	33 800	95 800	2.83	118	378
P5 (G1-OXDCAZ)	21 100	40 900	1.93	95	394
P6 (G2-OXDCAZ)	20 200	42 900	2.12	85	410

[a] Molecular weight determined by GPC in THF, based on polystyrene standards. [b] Glass transition temperature (°C) determined by DSC at a heating rate of 10 °C min^{-1}. [c] Temperature (°C) at 5% weight loss measured by TGA at a heating rate of 20 °C min^{-1} under nitrogen.

Scheme 1. The attachment of compounds **1**−**3** to 2,7-dibromofluorene was done by following a literature procedure[11c] with THF as a solvent, aqueous KOH as a base, and triethylbenzylammonium chloride (TEBAC) as a phase transfer catalyst (PTC). Pure monomers **M1**−**M3** were confirmed by ^{1}H NMR, elemental analyses, and FAB (or MALDI−TOF) mass spectroscopy. The dendronized polymers P1−P6 were synthesized from a Suzuki coupling reaction in a biphasic system (toluene/aqueous K_2CO_3) with freshly prepared Pd{P(*p*-tolyl)$_3$}$_3$ as a catalyst precursor.[28] In the beginning, when Pd(PPh_3)$_4$ is used as a catalyst precursor, the G2-substituted polymer (**P3** and **P6**) cannot be obtained due to the bulky side group of **M3** (**6**) to hide the reactive site, where Pd{P(*p*-tolyl)$_3$}$_3$ seems to be a superior choice in many SPC cases.[29] Copolymers **P4**−**P6** containing hole-transporting CAZ pendent groups were also synthesized to compare with those polymer counterparts without CAZ pendants (**P1**, **P2**, and **P3**). Standard workup afforded the dendronized polymers **P1**−**P6** as amorphous, slightly yellow materials. All polymers could be fully dissolved in common organic solvents, such as dichloromethane, chloroform, and THF. The molecular weights determined by GPC against polystyrene standards are summarized in Table 1. These data show that considerable molecular weights were achieved in these dendronized polymers, which have number-average molecular weights (M_n) ranging 20200−34500 with polydispersity indices (M_w/M_n) of 1.36−2.97.

The thermal stability of the polymers was determined by thermogravimetric analysis (TGA) under nitrogen. All polymers exhibited degradation temperatures (T_d) higher than 370 °C (5% weight loss under nitrogen). The degradation patterns of these polymers are quite similar, which possess a main weight loss step at the onset temperatures of T_d in the range of 430−450 °C. Phase transition temperatures of the polymers were also investigated by differential scanning calorimetry (DSC) under nitrogen. Though poly(fluorene)s usually reveal a crystallization temperature due to their crystalline nature in the solid state, DSC curves showed no crystallization and melting peaks but only glass transition temperatures (T_gs) in polymers **P1**−**P6** (as shown in Figure 1 of the Supporting Information). This obviously indicates that the presence of OXD and CAZ units in these copolymers suppresses the crystallinity and chain aggregation of the polymers effectively. The T_gs of the polymers are in the range of 85−143 °C and gradually drop by increasing the size of the dendritic OXD wedges, i.e., **P1** > **P2** > **P3** and **P4** > **P5** > **P6**. However, the copolymers containing CAZ pendent units (**P4**, **P5**, and **P6**) have lower glass transition temperatures (T_gs) than those polymer counterparts without CAZ pendants (**P1**, **P2**, and **P3**), respectively, which might be due to the longer spacer length in CAZ side chains.

Optical Properties. The absorption and PL data of dendritically functionalized polymers **P1**−**P6** were measured in both solution and solid states, and the optical properties are summarized in Table 2. As shown in Figure 1, the intensities of the

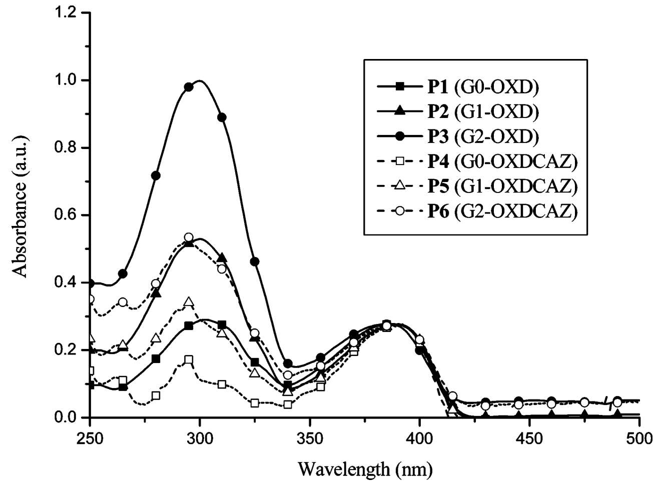

Figure 1. Absorption spectra of polymers **P1**−**P6** in THF solutions, normalized at the absorption peak of the polymer backbone.

short-wavelength absorption peaks (at ca. 300 nm) in THF solutions of **P1**−**P3** increase with the generation number of the dendrons, which are attributed to the absorption of the peripheral OXD units. Similarly, the absorption band of **P4**−**P6** solutions (in THF) at ca. 295 nm are originated from the combined absorption band of OXD and CAZ pendent groups (as shown in Figure 2 of the Supporting Information). The additional absorption bands of polymers **P1**−**P6** at 384−391 nm are assigned to the $\pi-\pi^*$ transition contributed from the conjugated backbones of the poly(fluorene)s. The absorption spectra of the polymers in solid films are similar (a little red-shifted) to those in THF solutions (as shown in Figure 3 of the Supporting Information). Optical band gaps (E_g) determined from the absorption edge of **P1**−**P6** in solid films are found to be about 2.94 eV. As shown in Figure 2, the PL spectra of polymers in THF solutions are quite similar to one another. All polymers emit blue light at 417 nm with vibronic bands at 441 nm (except **P3**, which reveals two sharp bands at 415 and 439 nm). The slightly blue-shifted spectrum of **P3** could be explained by the incorporation of the attachment of G2-bulky OXD dendrons onto the side chains of the fluorene units, which twist the poly(fluorene) backbones to decrease the effective conjugation length to some extent. The PL spectra of polymers in solid films are similar to those in THF solutions in Figure 2. In comparison with the corresponding dilute solutions, the emission spectra of **P1**−**P6** in solid films show a slight red-shift of 8−11 nm (Figure 3). Similar to the solution state, the PL spectrum of **P3** in the solid state is slightly blue-shifted relative to the other polymers. It is worth noticing that the PL spectra of **P1** and **P4** have a long tail extending to longer wavelength regions (the "onsets" of the longer wavelength region is at 610 nm) and show a shoulder at ca. 520 nm. This spectral feature is attributed to the interchain excimer formation and/or keto defects, which is commonly observed in 9,9-disubstituted poly(fluorene)s.[30−32] It appears that the G0-substituent is not bulky enough to shield the polymer backbones completely. The incomplete suppression of long wavelength emission band were also seen in similar dendronized poly(fluorene)s with smaller dendrons.[11(c)] However, **P2**, **P3**, **P5**, and **P6** with larger dendrons do not show any sign of aggregation or excimer formation. These results clearly indicate that the steric hindrance of larger dendritic substituents suppresses the intermolecular $\pi-\pi$ stacking of the polymers and eliminates undesirable red-shifts in the emission spectra.

It is already known that OXD and CAZ units can act as energy-transfer donors (light antennae) for the light-emitting

CDV

Table 2. Absorption and PL Emission Spectral Data of Polymers in THF Solutions and Solid Films

polymer	$\lambda_{abs,sol}{}^{a}$ (nm)	band gap (eV)	$\lambda_{PL,sol}{}^{a}$ (nm)	$\lambda_{PL,film}{}^{a}$ (nm)	$\Phi_{PL,sol}{}^{b}$	$\Phi_{PL,film}{}^{c}$
P1 (G0-OXD)	302, 387	2.94	417, 441	426, 449	0.73	0.34
P2 (G1-OXD)	300, 391	2.94	417, 441	427, 449	0.98	0.55
P3 (G2-OXD)	299, 384	2.94	415, 439	423, 445	0.77	0.16
P4 (G0-OXDCAZ)	295, 391	2.94	417, 441	427, 448	0.97	0.30
P5 (G1-OXDCAZ)	295, 391	2.94	417, 441	428, 449	1.00	0.52
P6 (G2-OXDCAZ)	295, 388	2.94	417, 441	426, 448	0.86	0.24

[a] The data in parentheses are the wavelengths of shoulders and subpeaks. [b] Solution fluorescence quantum efficiency were measured in THF, relative to 9,10-diphenylanthracene ($\Phi_{PL} = 0.90$). [c] PL quantum efficiency were estimated relative to 9,10-diphenylanthracene in poly(methyl methacrylate) as a standard ($\Phi_{PL} = 0.83$).

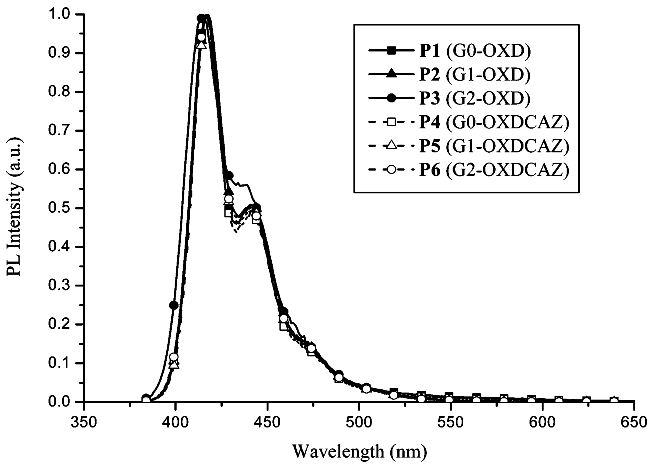

Figure 2. Normalized PL spectra of polymers **P1**−**P6** excited at the maximum absorption of backbones in THF solutions.

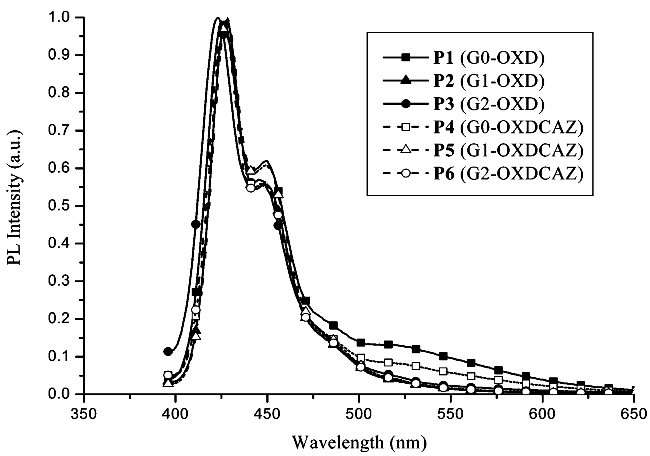

Figure 3. Normalized PL spectra of polymers **P1**−**P6** excited at the maximum absorption of backbones in solid films.

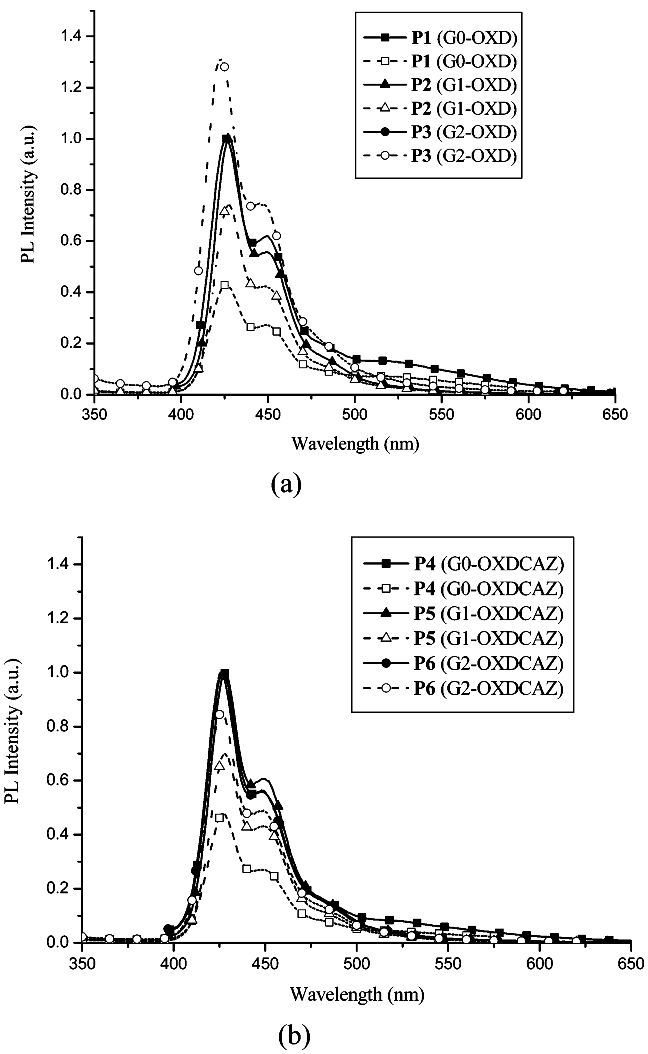

Figure 4. Normalized PL spectra of polymers (a) **P1**−**P3** and (b) **P4**−**P6** in solid films, which were excited at the maximum absorption of the peripheral OXD pendants (open symbols) and at the maximum absorption of the polymer backbone (solid symbols).

cores (as energy-transfer acceptors). In fact, the photoexcitations of OXD or CAZ units predominantly created identical emissions as those excited at the absorption of poly(fluorene) backbones. No characteristic emission features of OXD or CAZ side chains were observed in Figure 4, which indicate that both pendant groups (as energy-transfer donors) and polymer backbones (as energy-transfer acceptors) contribute the major emissions of the poly(fluorene)s. As shown in Figure 4(a), the intensity of the sensitized emission (excited at peripheral OXD units ca. 303 nm) of **P3** is 31% higher than the direct backbone emission (excited at the maximum absorption of the polymer backbone ca. 390 nm), which is the only enhanced result of the sensitized emission due to the largest number of dendritic OXD pendants (energy-transfer donors) in the highest generation of dendrons. The result clearly indicates that the photoluminescence of dendronized polymers by the light antenna design is more efficient than direct excitation at the absorption maximum of the polymer backbone. The PL quantum yields (Φ_{PL}) of polymers **P1**−**P6** excited at the maximum absorption of backbones in solutions were measured with 9,10-diphenylanthracene as a reference standard (cyclohexane, $\Phi_{PL} = 0.90$),[33] where the highest quantum yield reaches 1.0. The PL quantum yields in solid films were measured using the same standard in poly(methyl methacrylate),[34] and the results are listed in Table 2. The PL efficiencies of copolymers **P1**−**P3** show a trend similar to those of copolymers **P4**−**P6**, where the polymers incorporating smaller G0-substituted dendrons exhibit relatively higher degrees of aggregation and larger tendencies of excimer formation, and thus to possess relatively lower PL efficiencies. The G1-substituted polymers, however, exhibit the highest PL

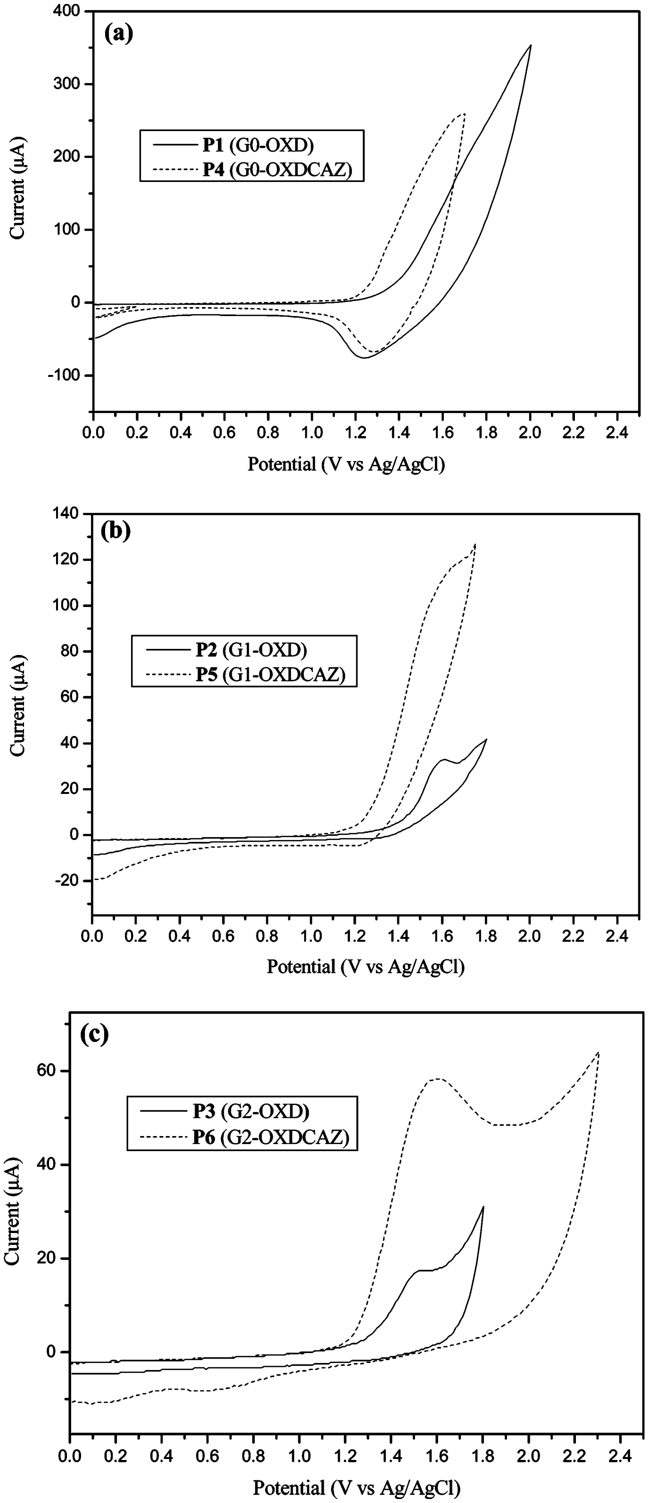

Figure 5. Cyclic voltammograms of the polymers: (a) **P1** and **P4**; (b) **P2** and **P5**; (c) **P3** and **P6**.

efficiencies with respect to their G0- and G2-analogues. The lower quantum yields of G2-analogues (**P3** and **P6**) with the highest generation of dendrons are probably due to the lower degrees of polymerization and slight twists of backbones in poly(fluorene) backbones, which lead to the quenching effect of poly(fluorene)s.

Electrochemical Characterization. Cyclic voltammetry (CV) measurements were carried out in a conventional three-electrode cell. The measured oxidation potentials and HOMO and LUMO energy values are summarized in Table 3. As

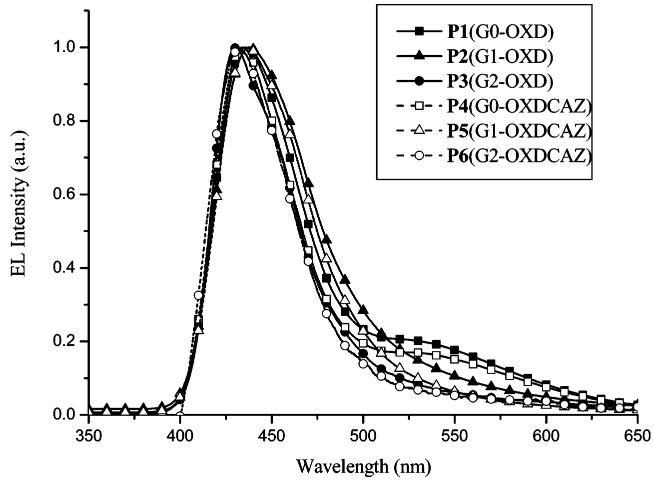

Figure 6. Normalized EL spectra of the devices with the configuration of ITO/PEDOT/polymer/LiF/Al.

Table 3. Oxidation Potentials and Calculated HOMO and LUMO Energies of Polymers

polymer	$E_{ox/onset}$ (V)	HOMO (eV)	LUMO[a] (eV)
P1 (G0-OXD)	1.37	−5.72	−2.78
P2 (G1-OXD)	1.38	−5.73	−2.79
P3 (G2-OXD)	1.32	−5.67	−2.73
P4 (G0-OXDCAZ)	1.23	−5.58	−2.64
P5 (G1-OXDCAZ)	1.26	−5.61	−2.67
P6 (G2-OXDCAZ)	1.24	−5.59	−2.65

[a] LUMO Energies were deduced from HOMO values and optical band gaps.

depicted in Figure 5, polymers **P1**−**P3** show the onset potentials of oxidation between 1.32 and 1.38 V in the anodic scans. The onset potentials are similar to the reported value of poly(2,7-(9,9-dioctyl)-fluorene)s (1.4 V)[35] and the onset potentials are due to the oxidation of the poly(fluorene) backbones. On the contrary, copolymers **P4**−**P6** have lower onset potentials of oxidation between 1.23 and 1.26 V, which are attributed to the introduction of CAZ groups.[36] It implies that the CAZ units reduce the hole-injection barrier by 0.08−0.14 eV thus to facilitate the capability of hole injection from ITO electrodes. Similarly, the high electron affinity of OXD units is helpful in electron injection. The HOMO energy values of **P1**−**P6** were calculated relative to ferrocene (Fc), which has a value of −4.8 eV with respect to zero vacuum level. In addition, the optical edges of absorption spectra are utilized to derive the band gaps and give the LUMO energy values of the dendronized polymers.[37] It can be visualized that the generation variety of the OXD dendrons has little effect on the oxidation potentials. The redox wave broadening or shifted effects on higher generations of dendrons, which were referred as the shell effect,[38] can be observed in G2-substituted polymers **P3** and **P6**.

Electroluminescent Properties. To evalutae these novel dendron-functionalized luminescent materials, double-layer light emitting devices using the dendronized polymers **P1**−**P6** as the active layer with the configuration of ITO/PEDOT/polymer/LiF/Al have been fabricated and investigated. The performance data of these devices are collected in Table 4. As a result, the emission wavelengths and spectral features of the EL spectra (Figure 6) are very similar to those of the corresponding PL spectra in solid films, which suggest that their EL emissions originate from the poly(fluorene) backbones. Both **P1** and **P4** show significantly broadened emissions to agree with their PL spectra, which might be due to excimer fromation by aggregation in the solid state or fluorenone defects introduced during

Table 4. EL Data of PLED Devices[a]

polymer	$\lambda_{max,EL}$ (nm)	V_{on}[b] (V)	power effiency[c] (cd/A)	luminance effiency[c] (lm/W)	max. brightness (cd/m^2)
P1 (G0-OXD)	436	5.0	0.90	0.31	1480
P2 (G1-OXD)	438	7.5	0.34	0.08	380
P3 (G2-OXD)	432	9.0	0.10	0.05	520
P4 (G0-OXDCAZ)	434	4.5	0.24	0.12	2446
P5 (G1-OXDCAZ)	438	7.0	0.10	0.02	119
P6 (G2-OXDCAZ)	432	8.5	0.05	0.02	92

[a] Device structure: ITO/PEDOT/polymer/LiF/Al. [b] V_{on} is the turn-on voltage of light. [c] Measured at 100 mA/cm^2.

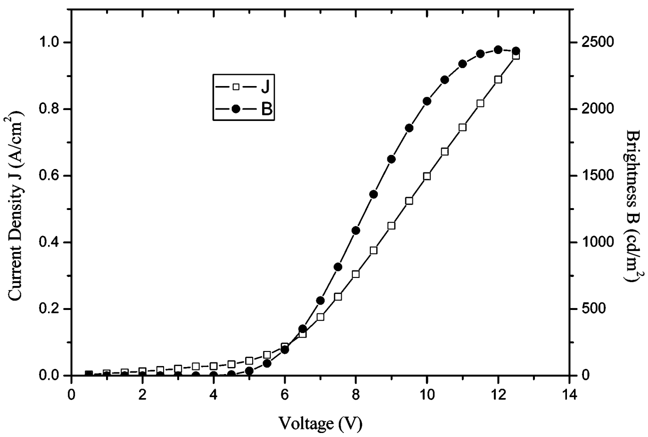

Figure 7. Current density−voltage-brightness (J−V−B) characteristics of the PLED device containing **P4** with the configuration of ITO/PEDOT/**P4**/LiF/Al.

device fabrication and operation.[5c,39,40] However, the green emission has been efficiently suppressed in **P2**, **P3**, **P5**, and **P6**, which might be due to the hindrance of the exciton migration to reduce oxidized ketonic defects by the bulky OXD dendrons and thereby to increase the color stability of these devices.[41] The PLED device made of **P4** (Figure 7) has the maximum brightness of 2446 cd/m^2 at a bias voltage of 12 V with a power efficiency of 0.24 cd/A at 100 mA/cm^2. The turn-on voltages of PLED devices based on G2-substituted polymers were a few volts higher than those of PLED devices based on G0- and G1-substituted polymers as shown in Table 4. Such unfavorable results are presumably due to a dominant shielding effect of G2-dendritic wedges, which deteriorates the charge transporting properties for the higher generations of the dendrimers.[42] The device performance characteristics of G0 dendritic PF-based PLEDs are generally better than those of corresponding G1 and G2 dendritic PF-based devices, which suggests that the larger dendron shells have a larger influence on the trapping process.[43]

Conclusion

A series of novel poly(fluorene)s containing three generations of dendronized side chains, including Fréchet-type poly(aryl ether) dendrons and functional peripheral groups such as OXD units were synthesized. The resulting polymers possess good thermal stability and excellent solubility in common organic solvents. The G1- and G2-substituted polymers may narrow down the emission spectra by reducing the emission spectral tail (extending to longer wavelength regions). The improvement of the emission spectral quality is attributed to less molecular packing caused by the steric hindrance of bulky dendritic side chains. The PLEDs with the configuration of ITO/PEDOT/polymer/LiF/Al were fabricated, and emitted blue light. The poor device performance of the more bulky dendronized poly(fluorene)-based PLEDs are presumably due to a large excess of the electron-affinitive OXD moieties in the higher generations of dendrons, which could act as electron traps and lead to the reduction of charge balance.

Acknowledgment. We express thanks for the financial support from the National Science Council of Taiwan (ROC) through NSC 93-2113-M-009-011. Prof. Yu-Tai Tao (vacuum deposition) at Institute of Chemistry, Academia Sinica (in Taiwan) and Prof. Chain-Shu Hsu (CV measurements), Prof. Yu-Chie Chen (MALDI−TOF mass spectroscopy), and Prof. Ching-Fong Shu (GPC measurements) at Department of Applied Chemistry, National Chiao Tung University (in Taiwan) are also acknowledged for their instrumental support.

Supporting Information Available: Text giving the preparations of compounds **1**−**3** and their intermediates, a scheme showing this, and figures showing the absorption spectra of polymers in solid films and DSC thermograms of polymers. This material is available free of charge via the Internet at http://pubs.acs.org.

References and Notes

(1) (a) *Handbook of Conducting Polymers*, 2nd ed.; Skotheim, T. A., Ed.; Dekker: New York, 1997. (b) *Conjugated Conducting Polymers*; Kies, H., Ed.; Springer: Berlin, 1992; Vol. 102. (c) Miller, J. S. *Adv. Mater.* **1993**, *5*, 671. (d) Roncali, J. *Chem. Rev.* **1992**, *92*, 711.

(2) (a) Pei, Q.; Yang, Y. *J. Am. Chem. Soc.* **1996**, *118*, 7416. (b) Leclerc, M. *J. Polym. Sci., Part A: Polym. Chem.* **2001**, *22*, 1365. (c) Grice, A. W.; Bradeley, D. D. C.; Bernius, M. T.; Inbasekaran, M.; Wu, W. W.; Woo, E. P. *Appl. Phys. Lett.* **1998**, *73*, 629.

(3) (a) Huber, J.; Müllen, K.; Salbeck, J.; Schenk, H.; Scherf, U.; Stehlin, T.; Stern, R. *Acta Polym.* **1994**, *45*, 244. (b) Lemmer, U.; Heun, S.; Mahrt, R. F.; Scherf, U.; Hopmeier, M.; Sieger, U.; Göbel, E. O.; Müllen, K.; Bässler, H. *Chem. Phys. Lett.* **1995**, *240*, 373. (c) Grell, M.; Bradley, D. D. C.; Ungar, G.; Hill, J.; Whitehead, K. S. *Macromolecules* **1999**, *32*, 5810.

(4) Jenekhe, S. A.; Osaheni, J. A. *Science* **1994**, *265*, 765.

(5) (a) List, E. J. W.; Güntner, R.; Scanducci de Freitas, P.; Scherf, U. *Adv. Mater.* **2002**, *14*, 374. (b) Gong, X.; Iyer, P. K.; Moses, D.; Bazan, G. C.; Heeger, A. J.; Xiao, S. S. *Adv. Funct. Mater.* **2003**, *13*, 325. (c) Scherf, U.; List, E. J. M. *Adv. Mater.* **2002**, *14*, 477.

(6) (a) Lee, J. I.; Klarner, G.; Miller, R. D. *Chem. Mater.* **1999**, *11*, 1083. (b) Klarner, G.; Lee, J. I.; Davey, M. H.; Miller, R. D. *Adv. Mater.* **1999**, *11*, 115.

(7) Xiao, S.; Nguyen, M.; Gong, X.; Cao, Y.; Wu, H.; Moses, D.; Heeger, A. J. *Adv. Funct. Mater.* **2003**, *13*, 25.

(8) Yu, W. L.; Pei, J.; Huang, W.; Heeger, A. J. *Adv. Mater.* **2000**, *12*, 828.

(9) Zeng, G.; Yu, W. L.; Chua, S. J.; Huang, W. *Macromolecules* **2002**, *35*, 6907.

(10) (a) Marsitzky, D.; Murry, J.; Scott, J. C.; Carter, K. R. *Chem. Mater.* **2001**, *13*, 4285. (b) Cho, H. J.; Jung, B. J.; Cho, N. S.; Lee, J.; Shim, H. K. *Macromolecules* **2003**, *36*, 6704.

(11) (a) Setayesh, S.; Grimsdale, A. C.; Weil, T.; Enkelmann, V.; Müllen, K.; Meghdadi, F.; List, E. J. W.; Leising, G. *J. Am. Chem. Soc.* **2001**, *123*, 946. (b) Hawker, C. J.; Fréchet, J. M. J. *J. Am. Chem. Soc.* **1990**, *112*, 7638. (c) Marsitzky, D.; Vestberg, R.; Blainey, P.; Tang, B. T.; Hawker, C. J.; Carter, K. R. *J. Am. Chem. Soc.* **2001**, *123*, 6965. (d) Tang, H. Z.; Fujiki, M.; Zhang, Z. B.; Torimitsu, K.; Motonaga, M. *Chem. Commun.* **2001**, 2426. (e) Chou, C. H.; Shu, C. F. *Macromolecules* **2002**, *35*, 9673.

(12) (a) List, E. J. W.; Guentner, R.; de Freitas, P. S.; Scherf, U. *Adv. Mater.* **2002**, *14*, 374. (b) Gaal, M.; List, E. K. W.; Scherf, U. *Macromolecules* **2003**, *36*, 4236. (c) Craig, M. R.; Kok, M. M.; Hofstraat, J. W.; Schenning, A. P. H. J.; Meijer, E. W. *J. Mater. Chem.* **2003**, *13*, 2861. (d) Kulkarni, A. P.; Kong, X.; Jenekhe, S. A. *J. Phys. Chem. B* **2004**, *108*, 8689.

(13) (a) Liu, M. S.; Jiang, X.; Liu, S.; Herguth, P.; Jen, A. K. Y. *Macromolecules* **2002**, *35*, 3532. (b) Jenekhe, S. A.; Osaheni, J. A. *Science* **1994**, *265*, 765.

(14) Krebs, F. C.; Jorgensen, M. *Macromolecules* **2002**, *35*, 7200.

(15) Chen, Z. K.; Meng, H.; Lai, Y. H.; Huang, W. *Macromolecules* **1999**, *32*, 4351.

(16) (a) Marsella, M. J.; Fu, D. K.; Swager, T. M. *Adv. Mater.* **1995**, *7*, 145. (b) Gillissen, S.; Jonforsen, M.; Kesters, E.; Johansson, T.; Theander, M.; Andersson, M. R.; Inganas, O.; Lutsen, L.; Vanderzande, D. *Macromolecules* **2001**, *34*, 7294.

CDV

(17) (a) Du, P.; Zhu, W. H.; Xie, Y. Q.; Zhao, F.; Ku, C. F.; Cao, Y.; Chang, C. P.; Tian, H. *Macromolecules* **2004**, *37*, 4387. (b) Pan, J.; Zhu, Zhu, W.; Li, S.; Zeng, W.; Cao, Y.; Tain, H. *Polymer* **2005**, *46*, 7658. (c) Liu, Y.; Yu, G.; Li, H.; Tian, H. Zhu, D. *Thin Solid Films* **2002**, *417*, 206. (d) Pan, J.; Zhu, W.; Li, S.; Xu, J.; Tian, H. *Eur. J. Org. Chem.* **2006**, 986.
(18) (a) Wang, C.; Jung, G. Y.; Hua, Y.; Pearson, C.; Bryce, M. R.; Petty, M. C.; Batsanov, A. S.; Goeta, A. E.; Howard, J. A. K. *Chem. Mater.* **2001**, *13*, 1167. (b) Zhan, X.; Liu, Y.; Wu, X.; Wang, S.; Zhu, D. *Macromolecules* **2002**, *35*, 2529. (c) Lee, Y. Z.; Chen, X.; Chen, S. A.; Wei, P. K.; Fann, W. S. *J. Am. Chem. Soc.* **2001**, *123*, 2296. (d) Peng, Z.; Zhang, J. *Chem. Mater.* **1999**, *11*, 1138. (e) Chung, S. J.; Kwon, K. Y.; Lee, S. W.; Jin, J. L.; Lee, C. H.; Lee, C. E.; Park, Y. *Adv. Mater.* **1998**, *10*, 1112. (f) Kim, J. H.; Park, J. H.; Lee, H. *Chem. Mater.* **2003**, *15*, 3414.
(19) Adachi, C.; Tsutsui, T.; Saito, S. *Appl. Phys. Lett.* **1990**, *56*, 799.
(20) Shu, C. F.; Dodda, R.; Wu, F. I.; Liu, M. S.; Jen, A. K. Y. *Macromolecules* **2003**, *36*, 6698.
(21) Wu, F. I.; Reddy, D. S.; Shu, C. F.; Liu, M. S.; Jen, A. K. Y. *Chem. Mater.* **2003**, *15*, 269.
(22) Sung, H. H.; Lin, H. C. *Macromolecules* **2004**, *37*, 7945.
(23) Kwok, C. C.; Wong, M. S. *Macromolecules* **2001**, *34*, 6821.
(24) Kwok, C. C.; Wong, M. S. *Chem. Mater.* **2002**, *14*, 3158.
(25) Sung, H. H.; Lin, H. C. *J. Polym. Sci., Part A: Polym. Chem.* **2005**, *43*, 2700.
(26) Ranger, M.; Rondeau, D.; Leclerc, M. *Macromolecules* **1997**, *30*, 7686.
(27) Wu, C. W.; Lin, H. C. *Macromolecules*, Submitted (**2006**).
(28) Tolman, C. A.; Seidel, W. C.; Gerlach, D. H. *J. Am. Chem. Soc.* **1972**, *94*, 2669.
(29) (a) Frahn, J.; Karakaya, B.; Schäfer, A.; Schlüter, A. D. *Tetrahedron* **1997**, *53*, 15459. (b) Schlüter, S.; Frahn, J.; Schlüter, A. D. *Macromol. Chem. Phys.* **2000**, *201*, 139.
(30) (a) Kreyenschmidt, M.; Klaemer, G.; Fuhrer, T.; Ashenhurst, J.; Karg, S.; Chen, W. D.; Lee, V. Y.; Scott, J. C.; Miller, R. D. *Macromolecules* **1998**, *31*, 1099. (b) Bliznyuk, V. N.; Carter, S. A.; Scott, J. C.; Klärmer, G.; Miller, R. D.; Miller, D. C. *Macromolecules* **1999**, *32*, 361.(c) Sims, M.; Bradley, D. D. C.; Ariu, M.; Koeberg, M.; Asimakis, A.; Grell, M.; Lidzey, D. G. *Adv. Funct. Mater.* **2004**, *14*, 765.
(31) Lee, J. I.; Klaerner, G.; Miller, R. D. *Chem. Mater.* **1999**, *11*, 1083.
(32) Jenekhe, S. A.; Osaheni, J. A. *Science* **1994**, *265*, 765.
(33) Eaton, D. *Pure Appl. Chem.* **1998**, *60*, 1107.
(34) Guilbault, G. G., Ed. *Practical Fluorescence*; Marcel Dekker: New York, 1990; Chapter 1.
(35) Janietz, S.; Bradley, D. D. C.; Grell, M.; Giebeler, C.; Inbasekaran, M.; Woo, E. P. *Appl. Phys. Lett.* **1998**, *73*, 2453.
(36) Xia, C.; Advincula, R. C. *Chem. Mater.* **2001**, *13*, 1682.
(37) Hohle, C.; Hofmann, U.; Schloter, S.; Thelakkat, M.; Strohriegl, P.; Haarer, D.; Zilker, S. J. *J. Mater. Chem.* **1999**, *9*, 2205.
(38) Satoh, N.; Cho, J. S.; Higuchi, M.; Yamamoto, K. *J. Am. Chem. Soc.* **2003**, *125*, 8104.
(39) Setayesh, S.; Grimsdale, A. C.; Weil, T.; Enkelmann, V.; Müllen, K.; Meghdadi, F.; List, E. J. W.; Leising, G. *J. Am. Chem. Soc.* **2001**, *123*, 946.
(40) Kraft, A.; Grimsdale, A. C.; Holmes, A. B. *Angew. Chem., Int. Ed.* **1998**, *37*, 402.
(41) Pogantsch, A.; Wenzel, F. P.; List, E. J. W.; Leising, G.; Grimsdale, A. C.; Mullen, K. *Adv. Mater.* **2002**, *14*, 1061.
(42) Lupton, J. M.; Samuel, I. D. W.; Beavington, R.; Burn, P. L.; Bässler, H. *Adv. Mater.* **2001**, *13*, 258.
(43) Qu, J.; Zhang, J.; Grimsdale, A. C.; Müllen, K.; Jaiser, F.; Yang, X.; Neher, D. *Macromolecules* **2004**, *37*, 8297.

MA060743Q